GREEN SYNTHESIS OF TERMINALIA ARJUNA-MEDIATED SELENIUM NANOPARTICLES: CHARACTERISATION AND IN-VITRO EVALUATION OF NANOGEL FOR ENHANCED WOUND HEALING

Dr. R.Vijayalakshmi 1*, Dr. N.Ambalavanan 2, Dr. S.Rajeshkumar 3, Dr. Jaideep Mahendra 4, Dr. Uma Sudhakar 5

¹ Professor, Department of Periodontology, Meenakshi Ammal Dental College & Hospital, Faculty of Dentistry, Meenakshi Academy of Higher Education and Research, Maduravoyal, Chennai, Tamil Nadu, India.

Email ID: drvijaya.perio@madch.edu.in, ORCID ID: https://orcid.org/0000-0002-8653-9642

² Professor Emeritus, Department of Periodontology, Meenakshi Ammal Dental College & Hospital, Faculty of Dentistry, Meenakshi Academy of Higher Education and Research, Maduravoyal, Chennai, Tamil Nadu, India. Email ID: profhod.perio@madch.edu.in, ORCID ID: https://orcid.org/0000-0002-0628-3959

³ Professor, Chief Scientist, Nanobiomedicine lab Saveetha dental college & Hospital SIMATS Saveetha University Chennai, Tamil Nadu, India. Email ID: rajeshkumars.sdc@saveetha.com, ORCID ID: https://orcid.org/0000-0001-7059-8894

⁴ Professor and Head, Department of Periodontology, Meenakshi Ammal Dental College & Hospital, Faculty of Dentistry, Meenakshi Academy of Higher Education and Research, Maduravoyal, Chennai, Tamil Nadu, India. Email ID: jaideep_m_23@yahoo.co.in, ORCID ID: https://orcid.org/0000-0002-4726-3727

⁵ Professor and Head, Department of Periodontology, Thai Moogambigai Dental College and Hospital Nerkundram, Chennai, Tamil Nadu, India. Email ID: ums_570@yahoo.co.in, ORCID ID: https://orcid.org/0000-0002-3179 Corresponding Author: Dr. R.Vijayalakshmi

Abstract

Introduction: This study aims to investigate the green synthesis of selenium nanoparticles (SeNPs) using *Terminalia arjuna* and assess their potential application in wound healing. The research explores the distinctive characteristics of SeNPs, such as their crystalline nature and complex composition, with the ultimate goal of contributing to advancements in nanomedicine and wound care.

Methods: X-ray diffraction (XRD) analysis confirmed the crystalline nature of SeNPs, revealing a nuanced structural complexity with both crystalline and amorphous components. Fourier-Transform Infrared (FTIR) Spectroscopy identified specific functional groups, further affirming SeNP formation. Scanning Electron Microscopy (SEM) showcased a prevalent nanoaggregate structure, suggesting potential applications in nanomedicine and catalysis.

Results: The calculated crystallite size of 30 nanometers, determined by the Debye-Scherrer equation, indicated a uniform size distribution within the SeNP ensemble. The SEM imaging highlighted the tendency of SeNPs to cluster, emphasizing their potential in specific applications. The synthesized SeNPs were incorporated into a gel, exhibiting higher viscosity than the control group. Gel dispersion studies indicated suitability for controlled and sustained delivery. Cytotoxicity assessment on Human periodontal ligament fibroblast cells revealed concentration-dependent reduction in cell viability, underscoring potential cytotoxic effects. Cell morphological analysis demonstrated distinct alterations induced by the *T. arjuna* SeNPs nanogel, including enhanced cell migration, filopodia formation, and a spindle-like appearance. These changes suggested a potential influence on key cellular processes. In-vitro scratch wound healing assays provided compelling evidence of the therapeutic efficacy of the *T. arjuna* SeNPs nanogel. Treated cells exhibited accelerated wound closure, emphasizing the gel's potential in promoting wound healing processes.

Conclusion: The study successfully achieved its aim by providing a comprehensive exploration of SeNP synthesis and gel formulation. The observed effects on cellular processes and wound healing underscore the significant promise of SeNPs as a therapeutic antibacterial platform. The multifaceted attributes of the synthesized SeNPs and their gel formulation present a promising avenue for future exploration in advanced wound care and nanomedicine.

Keyword: Selenium nanoparticles, Green synthesis, Terminalia arjuna, Wound healing gel.

INTRODUCTION

Impaired wound healing poses a significant challenge in today's healthcare landscape, especially among the elderly population.

Factors such as aging, diabetes, atherosclerosis, and venous insufficiency contribute to the rising prevalence of chronic wounds [1]. Despite this, there is a notable lack of evidence-

based research and consensus regarding the most effective interventions for wound healing [2]. The field necessitates innovation not only in technological aspects but also in terms of data collection, assessment tools, diagnostics and therapeutic interventions [3]. Technological advances alone are insufficient; equal emphasis must be placed on system, service, and process innovation [4]. Furthermore, understanding the mechanisms underlying age-related impairments in healing is essential, given that normal skin undergoes characteristic changes with age, leading to altered wound healing processes in elderly individuals [5]. In addressing the challenges associated with wound healing, collaboration among stakeholders, comprehensive research, and a dual focus on technological and non-technological innovations are imperative.

Selenium nanoparticles (SeNPs) possess distinctive attributes that contribute to their efficacy in promoting wound healing. Notably, SeNPs exhibit responsiveness to yellow light, enhancing their antibacterial capabilities and demonstrating anti-inflammatory properties [3]. Combining SeNPs with biological membranes, such as those from red blood cells, further augments their stability, immune evasion, and circulation time, proving effective in the context of infectious wound healing [4]. Encapsulating SeNPs with polydopamine and incorporating indocyanine green results in a photoresponsive therapeutic antibacterial platform. When exposed to laser irradiation, this platform displays a high antibacterial rate and accelerates the wound healing process [5]. SeNPs also exhibit diverse therapeutic effects in medical applications, leveraging their exceptional biological and physical properties. They can serve as an effective carrier medium for therapeutic substances, enhancing the overall curative effects of drugs [6]. In previous research, chitosan-ZnO/SeNPs nanoparticle scaffolds have been developed, showcasing outstanding antibacterial effects. These scaffolds contribute to collagen synthesis, re-epithelialization, and rapid wound closure [7]. The multifaceted capabilities of SeNPs make them a promising component in the development of advanced wound healing strategies.

Terminalia arjuna (TA) stands out as a medicinal plant renowned for its distinctive features and applications in wound healing. The plant is rich in various phytochemicals, including flavonoids, polyphenols, triterpenoids, tannins, and glycosides, all of which contribute to its medicinal prowess. These compounds endow TA with antimicrobial, anti-inflammatory, and cell-stimulating properties, rendering it effective in the promotion of wound healing [8]. Notably, TA extracts play a key role in the formulation of Ropana Taila, a traditional Ayurvedic medicine specifically tailored for wound healing purposes [9].Moreover, the therapeutic properties of TA extend beyond wound healing, encompassing benefits for heart health, such as lipid-lowering and antithrombotic effects, which may further contribute to its efficacy in promoting overall wound healing [10]. In a notable advancement, TA extracts have been employed in the green synthesis of metallic nanoparticles, showcasing significant potential in the context of wound healing applications [11] [12].

In this present study, selenium nanoparticles were synthesized through the utilization of *Terminalia arjuna* bark extract. The synthesized nanoparticles underwent comprehensive characterization, and subsequently, they were formulated into a gel. The wound healing potential of this gel was assessed through MTT assay and scratch wound healing assay conducted on a fibroblast cell line. This study aims to evaluate the efficacy of the selenium nanoparticles derived from *Terminalia arjuna* bark extract in promoting wound healing.

MATERIALS AND METHODS

Preparation of Terminalia arjuna bark extract

In this study, *Terminalia arjuna* bark extract plays a dual role as both a reducing and capping agent in the synthesis of selenium nanoparticles (SeNPs). The preparation of the bark extract involved measuring precisely 3g of *Terminalia arjuna* powder, which was then added to 100 mL of distilled water. Subsequently, the mixture was subjected to controlled boiling using a heating mantle set at 60-70 °C for 20 minutes. After the boiling process, the extract was filtered through Whatman No:1 filter paper, yielding a purified extract ready for utilization in SeNP synthesis.

Green Synthesis of Selenium Nanoparticles:

The synthesis process utilized 20mM sodium selenite as the precursor. The accurate measurement of 20mM sodium selenite was combined with 50mL of distilled water in a conical flask. Subsequently, 50mL of the previously filtered *Terminalia arjuna* bark extract was introduced into the flask. The reaction mixture was continuously stirred on a magnetic stirrer at 700 rpm for an extended period of 48 hours to facilitate the synthesis of selenium nanoparticles. After synthesis, the SeNP solution underwent centrifugation at 8000 rpm for 10 minutes, effectively separating the pellet from the supernatant. The collected SeNP pellet was meticulously stored in an airtight Eppendorff tube.

Formulation of *Terminalia arjuna*-Mediated Selenium Nanoparticles (SeNPs) Wound Healing Gel:

The gel preparation involved dissolving 2.5g of Carboxymethylcellulose in 25mL of distilled water, and separately, 2.5g of Carbopol was dissolved in another 25mL of distilled water. After achieving a homogeneous mixture for each component, the two solutions were combined and thoroughly mixed using a homogenizer. Once complete homogenization was achieved, the prepared gel served as the base for formulating the SeNPs-based wound healing gel. To this gel, 100mg of SeNPs, were added and further mixed thoroughly using a homogenizer to ensure a uniform blend. The resultant greensynthesized SeNPs-based gel was stored in a refrigerator for subsequent evaluation studies.

Characterization:

The structural characteristics of the green-synthesized SeNPs were analyzed using an X-ray diffraction spectrophotometer, examining both crystalline and amorphous phases. Fourier Transform Infrared Spectroscopy (FT-IR) was employed to identify the functional groups present in the synthesized selenium nanoparticles solution. Furthermore, Scanning Electron Microscopy (SEM) was employed to explore surface morphology, specifically focusing on the shape of the synthesized nanoparticles.

Evaluation of Gel

pH Measurement

A precise amount of gel was weighed and dissolved in 100 mL of purified water. The pH of the resulting mixture was determined using a digital pH meter.

Viscosity Measurement

The viscosity of the formulation was evaluated without dilution using a Rheometer with a spindle 05 at a weight of 0.1 g.

Homogeneity Testing

The formulation was visually inspected to assess its uniformity. Additionally, its physical appearance and the presence of any aggregates were examined.

Cell line study

Chemicals:

DMEM F-12, antibiotics (streptomycin, penicillin), trypsin-EDTA, phosphate buffer saline (PBS), FBS (Fetal Bovine Serum) obtained from Gibco (Invitrogen, USA). MTT (3-(4,5-dimethylthiazol-2-yl)-2,5-diphenyl tetrazolium bromide) reagent and dimethyl sulfoxide (DMSO) sourced from Sigma Aldrich Chemicals Pvt Ltd, USA. All other reagents used in this study were of analytical grade.

Establishment of Human periodontal ligament fibroblast Primary Cells:

Tissues were obtained during the extraction of first or second premolars as part of normal orthodontic therapy. Before tissue collection, patients provided informed consent. Tissues (20mg–50mg) were kept in sterile saline solution for one to four hours, following sterilization protocols and processing in a biosafety cabinet. To reduce oral bacterial flora, tissues were washed 10 times in PBS. After washing, tissues were sliced into small fragments (1-2 mm2) using a surgical blade on a sterile Petri plate with culture media. The tissue fragments were plated onto 25 cm² tissue culture flasks and incubated undisturbed for 48 hours at 37°C in a humidified incubator with 5% CO₂. The medium was changed after 48 hours, and cells were expanded until a sufficient number was reached for experiments.

Cell Viability (MTT) Assay:

Human periodontal ligament fibroblast cells (5×103 cells/well) were plated in 96-well plates with DMEM media, 1X Antibiotic Solution, and 10% fetal bovine serum (Gibco). After washing with 1X PBS, cells were treated with *T. arjuna*-mediated SeNPs-based gel and incubated for 24 and 48 hours. MTT (0.5mg/mL) was added, and after a 4-hour incubation, formazan crystals were dissolved in DMSO. Color intensity was measured at 570nm using a microplate reader, and cell viability was calculated using the formula:

% cell viability = [O.D of treated cells/O.D of control cells] \times 100.

Cell Morphology:

Human periodontal ligament fibroblast cells (2x105) were plated in 6-well plates and treated with *T. arjuna*-mediated SeNPs-based gel for 24 hours. After treatment, cells were observed under an inverted phase contrast microscope after washing with PBS.

Scratch Wound Healing Assay:

Human periodontal ligament fibroblast cells (2×105 cells/well) were seeded onto six-well culture plates. A scratch wound was created using a $200\mu l$ tip, washed with PBS, and photographed. *T. arjuna*-mediated SeNPs-based gel ($40\mu g/ml$) was applied for 24 hours, and the wounded area was photographed using an inverted microscope. Experiments were repeated in triplicate for each treatment group.

RESULTS

1. X-Ray diffraction spectrophotometer

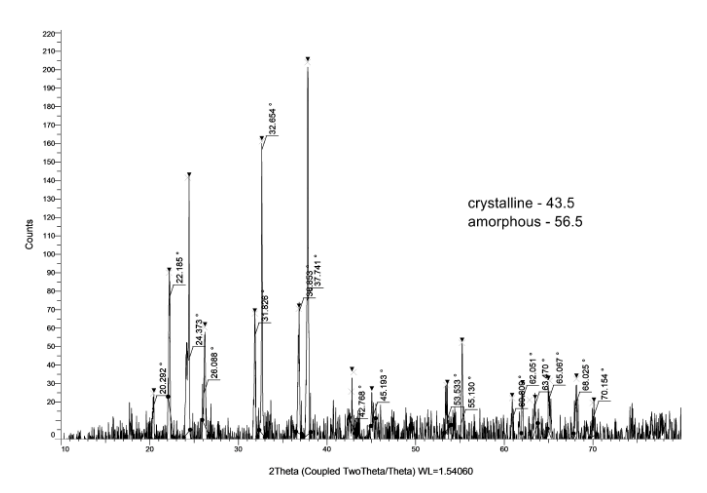


Figure 1: XRD spectrum of green synthesized selenium nanoparticles

The X-ray diffraction (XRD) spectrum depicted in Figure 1 exhibits well-defined peaks at 2θ angles of 20.292, 22.185, 24.873, 31.826, 36.863, and 37.741, underscoring the crystalline nature of the synthesized selenium nanoparticles. The discernible peaks correspond to specific crystallographic planes of selenium, providing evidence of a structurally organized crystalline material. Quantitative analysis of the XRD data reveals that 43.5% of the overall composition is attributed to crystalline phases, whereas the remaining 56.5% presents an amorphous structure. This coexistence of crystalline and amorphous components imparts a nuanced structural complexity to the synthesized selenium nanoparticles. Moreover, employing the Debye-Scherrer equation for size estimation yielded a calculated crystallite size of 30 nanometers. This average size aligns with the observed crystalline peaks in the XRD spectrum and signifies a well-defined size distribution within the nanoparticle ensemble.

2. Fourier Transorm Infra-red spectroscopy

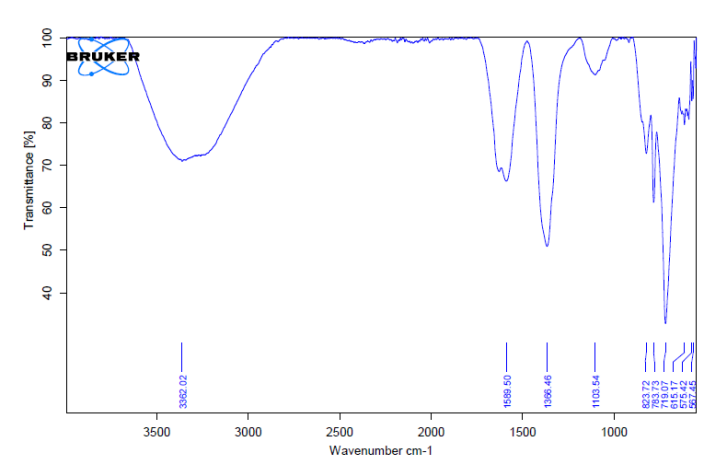


Figure 2: FTIR spectra *Terminalia arjuna* mediated selenium nanoparticles

The FTIR spectrum in Figure 2 showcases distinctive peaks at specific wavenumbers (3362.02, 1589.50, 1366.46, 1103.54, 823.72, 783.73, 719.07, 615.17, 575.42, 567.45). These peaks signify characteristic functional groups and molecular

vibrations. Notably, the peak at 3362.02 cm⁻¹ suggests the presence of hydroxyl groups, while the peak at 1589.50 cm⁻¹ indicates carbonyl groups. The peak at 1103.54 cm⁻¹ corresponds to the selenium-oxygen (Se–O) bond, confirming selenium nanoparticle formation. Additional peaks contribute to the complexity of the nanoparticle composition, potentially reflecting the involvement of various organic compounds from the plant extract.

3. Scanning Electron Microscope (SEM)

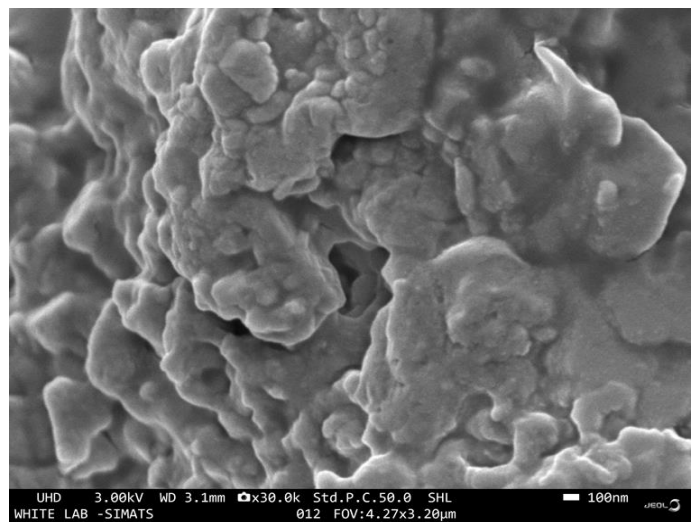


Figure 3: Scanning electron microscopic images of green synthesized selenium nanoparticles

The SEM images presented in Figure 3 revealed the morphology of selenium nanoparticles synthesized through a green approach. Notably, the predominant shape observed in these images is that of nanoaggregates. These nanoaggregates exhibit a distinctive irregular and interconnected structure, suggesting a tendency of individual selenium nanoparticles to cluster together. The green synthesis method employed in this study not only offers an environmentally friendly approach but also results in the formation of selenium nanoparticles characterized by a propensity for aggregation. The specific nanoaggregate morphology observed in these SEM images holds significance for potential applications in various fields, including nanomedicine and catalysis.

4. Evaluation of gel:





Figure 4:Evaluation of selenium nanoparticle gel viscosity and dispersion

The viscosity of the selenium nanoparticle (Se NP) gel, determined through viscometer analysis, exhibited a flow time of 1 minute and 30 seconds for 1 ml. The pH of the gel was recorded as 6.11. In comparison, the control group, consisting of an empty gel, demonstrated a shorter flow time of 30 seconds. This indicates that the selenium nanoparticle gel displayed a higher viscosity than the empty gel, suggesting a potential influence of the nanoparticles on the rheological properties of the gel. Furthermore, gel dispersion studies revealed that the selenium nanoparticle gel exhibited a moderate level of dispersion when compared to the control group. The controlled release of selenium nanoparticles within the gel matrix and the resultant moderate dispersion imply the potential suitability of the gel formulation for controlled and sustained delivery applications.

MTT assay:



Figure 5: The cytotoxic effects of *T.arjuna* SeNPs on Human periodontal ligament fibroblast cells

Upon exposure of Human periodontal ligament fibroblast cells to *Terminalia arjuna* mediated selenium nanoparticles (*T.arjuna* SeNPs) at concentrations ranging from 100 to 600 μg/mL for 24 hours, cell viability was assessed using the MTT assay. The control group maintained 100% cell viability at both 24 and 48 hours. Notably, lower concentrations (100 and 200 μg/mL) exhibited negligible cytotoxicity with approximately 100% cell viability at both time points. At 300 μg/mL, a mild reduction to 90% viability was observed at 24 hours, returning to 100% at 48 hours. Concentrations of 400 μg/mL resulted in 90% viability at 24 hours and 95% at 48 hours. Subsequently, at 500 μg/mL, viability decreased to 85% (24h) and 90% (48h), while the

highest concentration tested (600 μ g/mL) showed a more pronounced reduction, with cell viability at 83% (24h) and 80% (48h). Statistical analysis revealed significant differences compared to the control group (* p < 0.05), indicating a concentration-dependent cytotoxic effect of *T.arjuna* SeNPs on Human periodontal ligament fibroblast cells.

Cell morphology

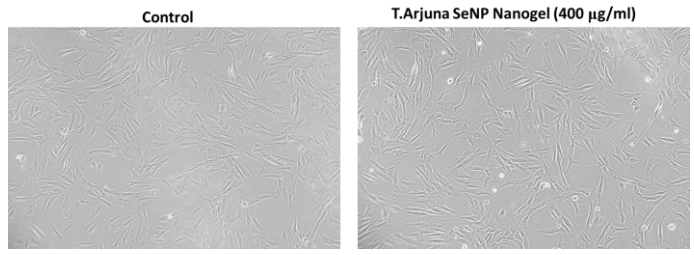


Figure 6: Cell morphological analysis. Human periodontal ligament fibroblast cells were treated with *T.arjuna* SeNP Nanogel (400 μ g/ml) for 24 h along with control group. Images were obtained using an inverted Phase contrast microscope.

Human periodontal ligament fibroblast cells treated with T.arjuna SeNP Nanogel at a concentration of 400 µg/mL for 24 hours were subjected to detailed cell morphological analysis using an inverted phase-contrast microscope, with the control group serving as a comparative reference. The microscopic examination revealed distinct alterations in cell morphology induced by the T.arjuna SeNP Nanogel treatment. Notably, treated cells exhibited a noticeable enhancement in cell migration compared to the control group after the 24-hour incubation period. The morphological changes included elongation of cell bodies, increased filopodia formation, and a more pronounced spindle-like appearance, indicative of heightened migratory activity. These findings suggest a potential role of T.arjuna SeNP Nanogel in modulating cellular morphology and migration, highlighting its significance in influencing key cellular processes. Representative images supporting these observations are presented in Figure 6, illustrating the morphological variations between the treated and control groups.

In vitro scratch wound healing assay

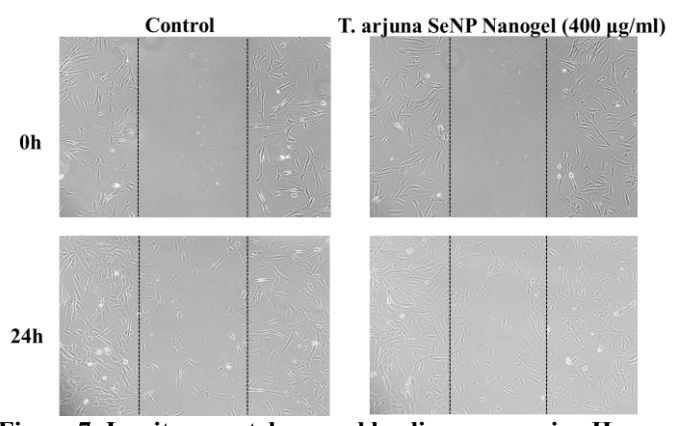


Figure 7: In-vitro scratch wound healing assay using Human periodontal ligament fibroblast cells treated with *T.arjuna* treated with SeNPs

In the in-vitro scratch wound healing assay, Human periodontal ligament fibroblast cells were subjected to an injury, and the subsequent cell migration response was assessed with and without treatment using T.arjuna SeNP Nanogel at a concentration of 400 µg/mL. The assay was conducted at 24 hours post-treatment, and images were captured using an inverted phase-contrast microscope. At the initial time point (0 hour), the control group exhibited no discernible cell migration, indicating the presence of the scratch wound. After 24 hours without treatment, the control group showed a limited degree of cell migration across the scratch wound. Contrastly, following treatment with T.arjuna SeNP Nanogel at 400 µg/mL, no cell migration was observed at the initial time point (0 hour), indicating a potential impact on the migratory response. Notably, at the 24-hour time point, the treated cells displayed a substantial enhancement in cell migration, evidenced by the increased coverage of the scratch wound area. These results suggest that T.arjuna SeNP nanogel at the specified concentration promotes accelerated in-vitro wound healing in Human periodontal ligament fibroblast cells. The images obtained using the inverted phase-contrast microscope visually corroborate the observed differences in cell migration between the treated and untreated groups, highlighting the potential therapeutic efficacy of *T.arjuna* SeNP Nanogel in promoting wound healing processes.

DISCUSSION

The present study encapsulates a comprehensive exploration of the green synthesis of selenium nanoparticles (SeNPs) facilitated by Terminalia arjuna, coupled with a thorough assessment of their application in wound healing through a specially formulated gel. The X-ray diffraction (XRD) analysis showcased distinct peaks at 20 angles, affirming the crystalline nature of the synthesized SeNPs. A structural complexity was revealed with the coexistence of crystalline and amorphous components, contributing 43.5% and 56.5%, respectively, to the overall composition. The Debye-Scherrer equation was employed to estimate a calculated crystallite size of 30 nanometers, aligning well with the observed crystalline peaks and indicating a uniform size distribution within the nanoparticle ensemble [13], [14]. Moving to the Fourier-transform infrared (FTIR) spectrum, characteristic peaks at specific wavenumbers unveiled the presence of hydroxyl groups, carbonyl groups, and selenium-oxygen (Se-O) bonds, reinforcing the confirmation of selenium nanoparticle formation. Additional peaks suggested the involvement of diverse organic compounds from the plant extract, contributing to the complex composition of the nanoparticles [15].

Scanning Electron Microscopic (SEM) imaging revealed the shape of the selenium nanoparticles to be prevalent nanoaggregate structure characterized by irregular and interconnected features. This distinctive morphology indicated a tendency of individual selenium nanoparticles to cluster, a noteworthy trait with potential applications in nanomedicine and catalysis [16]. The synthesized SeNPs were incorporated into a gel, and its viscosity was assessed using a viscometer, revealing a higher viscosity compared to the control group (empty gel). Gel dispersion studies further indicated a moderate level of dispersion, suggesting suitability for controlled and sustained delivery applications [17]. The cytotoxicity assessment on Human periodontal ligament fibroblast cells highlighted a concentration-dependent reduction in cell viability, with statistically significant differences compared to the control group. This underscores the potential cytotoxic effects of Terminalia arjuna-mediated selenium nanoparticles on these

cells. Cell morphological analysis, conducted with an inverted phase-contrast microscope, revealed distinct alterations induced by the *T.arjuna* SeNPs nanogel [18]. Treated cells exhibited enhanced cell migration, manifested by elongation of cell bodies, increased filopodia formation, and a more pronounced spindle-like appearance after a 24-hour incubation period, indicating a potential influence on key cellular processes [19], [20]. The in-vitro scratch wound healing assay provided compelling evidence of the therapeutic efficacy of *T.arjuna* SeNPs nanogel. Treated cells displayed accelerated wound closure, emphasizing the potential of the gel in promoting wound healing processes [21].

Selenium nanoparticles (SeNPs) exhibit promising potential in the field of wound healing. Numerous studies have highlighted their ability to enhance antibacterial properties, accelerate wound healing, and exhibit high efficiency in photothermal conversion [3], [7]. SeNPs have been successfully integrated into various scaffolds, such as chitosan-ZnO/SeNPs and polydopamine-functionalized SeNPs, demonstrating exceptional antibacterial effects against Escherichia coli and Staphylococcus aureus [22], [23]. Additionally, SeNPs have been combined with polyethylenimine and modified with indocyanine green for combined photoacoustic therapy. This approach proves effective in swiftly and safely eliminating drugresistant bacteria while promoting the healing of wounds [5]. Furthermore, researchers have encapsulated SeNPs with red blood cell membranes to improve their stability, immune evasion capabilities, and internal circulation time [24].

Overall, these findings collectively suggest that SeNPs hold significant promise as a therapeutic antibacterial platform for applications in wound healing. And these collectively underscore the multifaceted attributes of the synthesized selenium nanoparticles and their gel formulation, portraying a promising avenue for future exploration in advanced wound care and nanomedicine.

CONCLUSION

This study successfully synthesized selenium nanoparticles (SeNPs) using Terminalia arjuna, demonstrating their crystalline nature and structural complexity. The SeNPs, incorporated into a gel, exhibited increased viscosity, moderate dispersion, and promising potential for controlled delivery. Cytotoxicity assessments on human cells emphasized dosedependent effects, while cellular analysis morphological changes. Significantly, in-vitro wound healing assays demonstrated the therapeutic efficacy of the SeNPcontaining gel, indicating accelerated wound closure. These findings highlight the potential of SeNPs for advanced wound care applications.

References

- 1. M. Mieczkowski, B. Mrozikiewicz-Rakowska, M. Kowara, M. Kleibert, and L. Czupryniak, "The problem of wound healing in diabetes—from molecular pathways to the design of an animal model," Int. J. Mol. Sci., vol. 23, no. 14, p. 7930, Jul. 2022, doi: 10.3390/ijms23147930. Available: http://dx.doi.org/10.3390/ijms23147930
- 2. F. Gottrup, "Debridement: Another evidence problem in wound healing," Wound Repair Regen., vol. 17, no. 3, pp. 294–295, May 2009, doi: 10.1111/j.1524-475x.2009.00484.x. Available: http://dx.doi.org/10.1111/j.1524-475x.2009.00484.x
- 3. W. Huang et al., "Visible light-responsive selenium nanoparticles combined with sonodynamic therapy to

- promote wound healing," ACS Biomater. Sci. Eng., vol. 9, no. 3, pp. 1341–1351, Mar. 2023, doi: 10.1021/acsbiomaterials.2c01119. Available: http://dx.doi.org/10.1021/acsbiomaterials.2c01119
- 4. F. Davarani Asl, M. Mousazadeh, M. Azimzadeh, and M. R. Ghaani, "Mesoporous selenium nanoparticles for therapeutic goals: a review," J. Nanopart. Res., vol. 24, no. 10, Oct. 2022, doi: 10.1007/s11051-022-05572-7. Available: http://dx.doi.org/10.1007/s11051-022-05572-7
- 5. M. Sun et al., "Polydopamine-functionalized selenium nanoparticles as an efficient photoresponsive antibacterial platform," RSC Adv., vol. 13, no. 15, pp. 9998–10004, 2023, doi: 10.1039/d2ra07737j. Available: http://dx.doi.org/10.1039/d2ra07737j
- 6. X. Xiao et al., "Selenium nanoparticles: Properties, preparation methods, and therapeutic applications," Chem. Biol. Interact., vol. 378, no. 110483, p. 110483, Jun. 2023, doi: 10.1016/j.cbi.2023.110483. Available: http://dx.doi.org/10.1016/j.cbi.2023.110483
- 7. Q. Ruan et al., "Development of ZnO/selenium nanoparticles embedded chitosan-based anti-bacterial wound dressing for potential healing ability and nursing care after paediatric fracture surgery," Int. Wound J., vol. 20, no. 6, pp. 1819–1831, Aug. 2023, doi: 10.1111/iwj.13947. Available: http://dx.doi.org/10.1111/iwj.13947
- 8. V. Kumar et al., "Therapeutic potential and industrial applications of Terminalia arjuna bark," J. Ethnopharmacol., vol. 310, no. 116352, p. 116352, Jun. 2023, doi: 10.1016/j.jep.2023.116352. Available: http://dx.doi.org/10.1016/j.jep.2023.116352
- 9. A. G. Nerkar, R. K. Dumbre, and S. Badar, "Ethnopharmacological review of arjuna," Current Trends in Pharmacy and Pharmaceutical Chemistry, vol. 5, no. 1, pp. 21–25, Apr. 2023, doi: 10.18231/j.ctppc.2023.005. Available: http://dx.doi.org/10.18231/j.ctppc.2023.005
- 10. S. Yadav, S. Kaushik, S. Kumar Chhikara, S. Singh, J. Parkash Yadav, and S. Kaushik, "Terminalia arjuna (Arjun Tree): A Sacred plant with high Medicinal and Therapeutic Potential," Res. J. Pharm. Technol., pp. 5859–5867, Dec. 2022, doi: 10.52711/0974-360x.2022.00989. Available: http://dx.doi.org/10.52711/0974-360x.2022.00989
- 11. N. Shah, S. Mitra, U. Sharma, and K. Sharma, "Review on wound healing activity of Ropana Taila," Int. J. Ayurveda Pharma Res., pp. 13–21, Apr. 2022, doi: 10.47070/ijapr.v10i4.2274. Available: http://dx.doi.org/10.47070/ijapr.v10i4.2274
- 12. M. Tharani, S. Rajeshkumar, K. A. Al-Ghanim, M. Nicoletti, N. Sachivkina, and M. Govindarajan, "Terminalia chebula-Assisted Silver Nanoparticles: Biological Potential, Synthesis, Characterization, and Ecotoxicity," Biomedicines, vol. 11, no. 5, May 2023, doi: 10.3390/biomedicines11051472. Available: http://dx.doi.org/10.3390/biomedicines11051472
- 13. F. Martínez-Esquivias, M. D. Méndez-Robles, A. Villagómez-Vega, M. S. Segura-Almendárez, C. J. de la Cruz-Ahumada, and J. M. Guzman-Flores, "Medicinal applications of selenium nanoparticles synthesized by green methods," Lett. Org. Chem., vol. 21, no. 1, pp. 40–54, Jan. 2024, doi: 10.2174/1570178620666230727104849. Available:
 - http://dx.doi.org/10.2174/1570178620666230727104849
- 14. B. Nowruzi, B. S. Jalil, and J. S. Metcalf, "Antifungal screening of selenium nanoparticles biosynthesized by

- microcystin-producing Desmonostoc alborizicum," BMC Biotechnol., vol. 23, no. 1, p. 41, Sep. 2023, doi: 10.1186/s12896-023-00807-4. Available: http://dx.doi.org/10.1186/s12896-023-00807-4
- 15. A. S. Almurshedi et al., "New investigation of antiinflammatory activity of Polycladia crinita and biosynthesized selenium nanoparticles: isolation and characterization," Microb. Cell Fact., vol. 22, no. 1, p. 173, Sep. 2023, doi: 10.1186/s12934-023-02168-1. Available: http://dx.doi.org/10.1186/s12934-023-02168-1
- 16. A. H. Hashem et al., "Watermelon rind mediated biosynthesis of bimetallic selenium-silver nanoparticles: Characterization, antimicrobial and anticancer activities," Plants, vol. 12, no. 18, Sep. 2023, doi: 10.3390/plants12183288. Available: http://dx.doi.org/10.3390/plants12183288
- 17. C. Sivakumar and K. Jeganathan, "In-vitro cytotoxicity of java tea mediated selenium nanoballs against L6 cell lines," J. Drug Deliv. Ther., vol. 8, no. 6, pp. 195–200, Nov. 2018, doi: 10.22270/jddt.v8i6.2046. Available: http://dx.doi.org/10.22270/jddt.v8i6.2046
- 18. Y. Zhang, C. Ma, S. Zhang, C. Wei, Y. Xu, and W. Lu, "ROS-responsive selenium-containing polyphosphoester nanogels for activated anticancer drug release," Mater. Today Chem., vol. 9, pp. 34–42, Sep. 2018, doi: 10.1016/j.mtchem.2018.04.002. Available: http://dx.doi.org/10.1016/j.mtchem.2018.04.002
- 19. L. A. Pham-Huy, H. He, and C. Pham-Huy, "Free radicals, antioxidants in disease and health," Int. J. Biomed. Sci., vol. 4, no. 2, pp. 89–96, Jun. 2008, Available: https://www.ncbi.nlm.nih.gov/pubmed/23675073
- 20. P. J. Franks et al., "Randomized trial of cohesive short-stretch versus four-layer bandaging in the management of venous ulceration," Wound Repair Regen., vol. 12, no. 2, pp. 157–162, Mar. 2004, doi: 10.1111/j.1067-1927.2004.012206.x. Available: http://dx.doi.org/10.1111/j.1067-1927.2004.012206.x
- 21. D. Altememy, M. Javdani, P. Khosravian, A. Khosravi, and E. Moghtadaei Khorasgani, "Preparation of transdermal patch containing selenium nanoparticles loaded with doxycycline and evaluation of skin wound healing in a rat model," Pharmaceuticals (Basel), vol. 15, no. 11, p. 1381, Nov. 2022, doi: 10.3390/ph15111381. Available: http://dx.doi.org/10.3390/ph15111381
- 22. M. Fang, H. Zhang, Y. Wang, H. Zhang, D. Zhang, and P. Xu, "Biomimetic selenium nanosystems for infectious wound healing," Engineered Regeneration, vol. 4, no. 2, pp. 152–160, Jun. 2023, doi: 10.1016/j.engreg.2023.01.004. Available: http://dx.doi.org/10.1016/j.engreg.2023.01.004
- 23. P. Gao et al., "Ofloxacin-loaded selenium-tellurium nanoheterojunctions for skin infection and wound healing," May 22, 2023. doi: 10.22541/au.168475029.99475478/v1. Available:
 - http://dx.doi.org/10.22541/au.168475029.99475478/v1
- 24. M. Prasathkumar, C. Sakthivel, R. Becky, C. Dhrisya, I. Prabha, and S. Sadhasivam, "Phytofabrication of costeffective selenium nanoparticles from edible and non-edible plant materials of Senna auriculata: Characterization, antioxidant, antidiabetic, antimicrobial, biocompatibility, and wound healing," J. Mol. Liq., vol. 367, no. 120337, p. 120337, Dec. 2022, doi: 10.1016/j.molliq.2022.120337. Available: http://dx.doi.org/10.1016/j.molliq.2022.120337